Title

PDGFR-β modulates vascular smooth muscle cell phenotype via IRF-9/SIRT-1/NF-κB pathway in subarachnoid hemorrhage rats

Journal

Cerebrovascular and Brain Metabolism Reviews, 39(7)

ISSN

1040-8827

Authors

Wan, Weifeng
Ding, Yan
Xie, Zongyi
et al.

Publication Date

2019-07-01

DOI

10.1177/0271678x18760954

Peer reviewed

Original Article

JCBFM

Journal of Cerebral Blood Flow & Metabolism
2019, Vol. 39(7) 1369–1380

DOI: 10.1177/0271678X18760954
journals.sagepub.com/home/jcbfm
SAGE

PDGFR-β modulates vascular smooth muscle cell phenotype via IRF-9/SIRT-1/NF-κB pathway in subarachnoid hemorrhage rats

Weifeng Wan[1,2], Yan Ding[1], Zongyi Xie[1], Qian Li[1], Feng Yan[1], Enkhjargal Budbazar[1], William J Pearce[1], Richard Hartman[1], Andre Obenaus[1], John H Zhang[1], Yong Jiang[2] and Jiping Tang[1]

Abstract

Platelet-derived growth factor receptor-β (PDGFR-β) has been reported to promote phenotypic transformation of vascular smooth muscle cells (VSMCs). The purpose of this study was to investigate the role of the PDGFR-β/IRF9/SIRT-1/NF-κB pathway in VSMC phenotypic transformation after subarachnoid hemorrhage (SAH). SAH was induced using the endovascular perforation model in Sprague-Dawley rats. PDGFR-β small interfering RNA (siRNA) and IRF9 siRNA were injected intracerebroventricularly 48 h before SAH. SIRT1 activator (resveratrol) and inhibitor (EX527) were administered intraperitoneally 1 h after SAH induction. Twenty-four hours after SAH, the VSMC contractile phenotype marker α-smooth muscle actin (α-SMA) decreased, whereas the VSMC synthetic phenotype marker embryonic smooth muscle myosin heavy chain (Smemb) increased. Both PDGFR-β siRNA and IRF9 siRNA attenuated the induction of nuclear factor-κB (NF-κB) and enhanced the expression of α-SMA. The SIRT1 activator (resveratrol) preserved VSMC contractile phenotype, significantly alleviated neurological dysfunction, and reduced brain edema. However, these beneficial effects of PDGFR-β siRNA, IRF9 siRNA and resveratrol were abolished by the SIRT1 inhibitor (EX527). This study shows that PDGFR-β/IRF9/SIRT-1/NF-κB signaling played a role in the VSMC phenotypic transformation after SAH. Inhibition of this signaling cascade preserved the contractile phenotype of VSMCs, thereby improving neurological outcomes following SAH.

Keywords

Subarachnoid hemorrhage, vascular smooth muscle cell, phenotypic transformation, platelet-derived growth factor receptor-β, early brain injury

Received 28 July 2017; Revised 24 January 2017; Accepted 28 January 2018

Introduction

Aneurysmal subarachnoid hemorrhage (aSAH) leads to devastating outcomes in patients, including hydrocephalus, cerebral edema, neuronal apoptosis, cerebrovascular autoregulation disorder, microthrombosis, cortical spreading depression and cerebral vasospasm (CVS).[1–7] CVS is mainly due to increased vascular smooth muscle tone. Current treatments include vasodilatory calcium channel blockers (e.g. nimodipine and verapamil), but their effectiveness remains controversial.[8] However, vasodilatory drugs may be less effective when VSMCs have switched from the contractile phenotype to the synthetic phenotype in response to SAH during the early brain injury (EBI) phase.[9,10]

Under normal physiological conditions, VSMCs in the contractile phenotype play an essential role in

[1]Department of Physiology and Pharmacology, Loma Linda University, School of Medicine, Loma Linda, CA, USA
[2]Department of Neurosurgery, The Affiliated Hospital of Southwest Medical University, Luzhou, China

The first two authors contributed equally to this work.

Corresponding authors:
Yong Jiang, Department of Neurosurgery, The Affiliated Hospital of Southwest Medical University, Luzhou 646000, China.
Email: jiangyong@swmu.edu.cn
Jiping Tang, Loma Linda University, 11041 Campus Street, Loma Linda, California, USA.
Email: jtang@llu.edu

regulating vascular tone. Upon inflammatory stimuli, VSMCs take on the synthetic phenotype and have other functions crucial for long-term adaption, including proliferation, migration and synthesis of extracellular matrix (ECM).[11–13] However, synthetic VSMCs can further exacerbate vascular dysfunction and inflammation in the short term and increase vascular thickness and stiffness in the long term.[10] Our laboratory has found that inhibiting the VSMC phenotypic transformation after SAH attenuates EBI.[14] However, the underlying mechanisms remain largely unknown.

Previous studies have shown that platelet-derived growth factor receptor β (PDGFR-β) is expressed on cerebral VSMCs and has been involved in the pathogenesis of CVS after SAH.[15,16] Interferon regulatory factors 9 (IRF9) and silent information regulator transcript-1 (SIRT1) have been implicated as the downstream factors of PDGFR-β signaling in vascular injury.[17,18] Specifically, IRF9 was activated in VSMCs upon arterial injuries in vivo and was shown to be induced by PDGF-BB in vitro. IRF9 suppresses SIRT1 expression and activity. SIRT1 is a nicotinamide adenine dinucleotide (NAD)-dependent nuclear histone deacetylase that mainly plays an anti-inflammatory role in the vasculature by regulating proliferation and the cell cycle. One of its major deacetylation targets is nuclear factor-κB (NF-κB).[19] The acetylation of NF-κB and its proinflammatory program can lead to the induction of CyclinD1 and MMP-9 in the vasculature, which is associated with VSMC proliferation and migration.

In this study, we hypothesized that PDGFR-β/IRF9/SIRT1/NF-κB signaling mediates VSMC phenotypic transformation from the contractile phenotype to the synthetic phenotype after SAH, and that inhibition of PDGFR-β signaling would preserve contractile VSMCs. We evaluated the expression levels of α-smooth muscle actin (α-SMA), embryonic smooth muscle myosin heavy chain (Smemb) and Cyclin D1 to study VSMC phenotypic transformation.

Materials and methods

Animals

All experiments were conducted in compliance with the NIH Guidelines for the Use of Animals in Neuroscience Research. All experiments were approved by the Loma Linda University Institutional Animal Care and Use Committee. All experiments are reported in compliance with the ARRIVE (Animal Research: Reporting in Vivo Experiments) guidelines. Male adult Sprague-Dawley rats (body weight 280–320 g; Envigo, Livermore, CA) were housed in 12-h light/dark cycles at a controlled temperature and humidity with free access to food and water.

SAH model and experimental protocol

Endovascular perforation was produced in rats as described previously.[17] Briefly, rats were intubated transorally and mechanically ventilated throughout the whole operation period with 3% isoflurane anesthesia. A sharpened 4–0 monofilament nylon suture was inserted rostrally into the internal carotid artery from the external carotid artery stump and perforated the bifurcation of the anterior and middle cerebral arteries. Sham operated rats underwent the same procedures except that the suture was withdrawn without puncture.

Intracerebroventricular drug administration

Intracerebroventricular (i.c.v.) drug administration was performed as previously described.[20,21] Rats were placed in a stereotaxic apparatus under 2.5% isoflurane anesthesia, rectal temperature was maintained at 37.5°C using a feedback-controlled heating pad. A cranial burr hole (1 mm) was drilled in the skull 1.5 mm posterior and 1.0 mm lateral relative to bregma. The needle of a 10-μl Hamilton syringe (Microliter 701; Hamilton Company, Reno, NV) was inserted through the burr hole 3.2 mm below the horizontal plane of Bregma into the right lateral ventricle. PDGFR-β siRNA (100 μmol/L in 5 μl, OriGene), IRF9 siRNA (100 μmol/L in 5 μl; OriGene), or scrambled siRNA (100 μmol/L in 5 μl; OriGene) was infused at the rate of 0.5 μl/min 48 h before endovascular perforation/sham surgery. The needle was left in place for 5 min after injection to prevent reflux, and then it was slowly removed. The burr hole was then sealed with bone wax, and the incision was closed with sutures.

Severity of SAH

The severity of SAH was blindly assessed using a previously described grading scale at the time of euthanasia.[22] Briefly, animals were euthanized and the brains were removed. The basal cistern was divided into six segments. Each segment was allotted a grade from 0 to 3 depending on the amount of subarachnoid hemorrhage in the segment. The animals received a total score ranging from 0 to 18 after adding the score from all 6 segments. Rats that received a score less than 7 were excluded from this study.

Neurological outcome assessment

As previously reported, neurological impairment was blindly evaluated by an 18-point score system known as Modified Garcia Score at 24 h after SAH, including spontaneous activity, response to vibrissae touch, body proprioception, symmetry in the movement of all four

limbs, forepaw outstretching, and climbing, each subtest was given a score from 0 to 3. The beam balance test score from 0 to 4 was given according to the walking distance on a wide wooden beam for 1 min.[23]

Brain water content

Brain water content was measured as previously described.[14] Briefly, animals were euthanized, and their brains were removed 24 h after surgery. The brains were separated into left hemisphere, right hemisphere, cerebellum, and brain stem. Each part was weighed immediately after removal (wet weight). Brain specimens were then dried in an oven at 105°C for 72 h and weighed again (dry weight). The percentage of water content was calculated as follows: (wet weight – dry weight)/wet weight.

Western blot analysis

Western blot tests were performed as reported previously.[24,25] Briefly, animals were euthanized 24 h after SAH and perfused through the heart with cold phosphate-buffered (PBS, pH=7.4) solution, followed by removal of the brain. Circle of Willis blood vessels, basilar artery and cortical arteries were removed from the surface of the brain as reported previously.[14] The brain and vessel parts were stored appropriately at −80°C immediately until analysis. Protein extraction from whole-cell lysates of whole brain or vessels were obtained by gently homogenizing in RIPA lysis buffer (Santa Cruz) with further centrifugation at 14,000 at 4°C for 30 min. The supernatant was collected, and the protein concentration was measured using a detergent compatible assay (Bio-Rad, Dc protein assay). Equal amounts of protein were loaded on SDS-PAGE gels. After proteins were electrophoresed and transferred to nitrocellulose membranes, the membranes were blocked for 2 h at room temperature and incubated with the primary antibody overnight at 4°C. The primary antibodies included: rabbit monoclonal anti-PDGFR-β (1:2500, ab32570; Abcam), rabbit polyclonal anti-SIRT1 (1:400, sc-15404; Santa Cruz Biotechnology), rabbit polyclonal anti-IRF9 (1:200, sc-10793; Santa Cruz Biotechnology), rabbit polyclonal anti-NF-κB p65 (Acetyl-Lys310; 1:500, ab19870; Abcam), mouse monoclonal anti-smooth muscle actin (1:5000, sc-53015; Santa Cruz Biotechnology), rabbit monoclonal anti-CyclinD1 (1:1000, ab134175; Abcam), and goat polyclonal anti-actin (1:4000, sc-1616; Santa Cruz Biotechnology). The nitrocellulose membranes were incubated with secondary antibodies (Santa Cruz Biotechnology) for 2 h at room temperature. Immunoblots were probed with an ECL Prime Western Blotting Detection Reagent (Amersham; GE Healthcare), visualized with an imaging system (Bio-Rad, Versa Doc, model 4000), and analyzed using ImageJ software.

Immunofluorescence staining

Immunofluorescence staining was performed at 24 h after SAH as described previously.[20] Rats were perfused under deep anesthesia with cold PBS, then infused with 10% formalin. Pial arterioles with one or two layers of smooth muscle cells were chosen for the staining. Two or three arterioles were sampled from each animal. They were dissected and fixed in formalin at 4°C for 24 h. Samples were dehydrated with 30% sucrose at 4°C for 72 h. Sections (10 μm) were incubated overnight at 4°C with primary antibodies, including rabbit monoclonal anti-PDGFR-β (1:100, ab32570; Abcam), rabbit polyclonal anti-SIRT1 (1:100, sc-15404; Santa Cruz Biotechnology), rabbit polyclonal anti-IRF9 (1:50, sc-10793; Santa Cruz Biotechnology), mouse monoclonal anti-non-muscle Myosin IIB (Smemb; 1:100, ab684; Abcam), mouse monoclonal anti-smooth muscle actin (α-SMA; 1:50, sc-53015; Santa Cruz Biotechnology). It was then incubated with the appropriate fluorescence dye-conjugated secondary antibodies (Jackson Immunoresearch, West Grove, PA) in the dark room for 2 h at room temperature. The slices were visualized with a fluorescence microscope (DMi8; Leica Microsystems, Germany). Fluorescence intensity was quantified using ImageJ and presented as "Integrated Density".

Statistical analysis

Animals were all randomly assigned to different experimental groups. Endpoint assessments, such as neurobehavioral tests, Western blot and immunostaining, were performed by the investigators blinded to the group assignment. Parametric data were expressed as mean ± SEM. Statistical differences among groups were analyzed by using one-way ANOVA followed by Tukey post hoc test. For non-parametric data (*i.e.* neurological tests and SAH score), the data were analyzed with Kruskall–Wallis with Dunn's post hoc tests and also presented as mean ± SEM. P value of < 0.05 was considered significant difference. All statistical analysis was performed using GraphPad Prism software.

Results

Mortality and SAH severity scores

Experimental groups and mortality rate were listed in Supplemental Figures 1 and 2. The total mortality of SAH in this study was 15.7% (41 of 261 rats) and was

not significantly different between SAH animals sacrificed at different time points (3 h, 6 h, 12 h and 24 h). In addition, there was no significant difference in average SAH grading scores between SAH groups at different time points (Supplemental Figure 3).

PDGFR-β and its downstream factors were changed to a similar degree both in the vasculature and the left cerebral hemisphere after SAH

To examine whether the protein expression profile in the left hemisphere (LH) can be representative of the protein profile in the vasculature, we collected pial arterioles and LH protein lysates from both sham and SAH animals and compared the expression levels. PDGFR-β, IRF9, SIRT1, NF-κB, α-SMA and Cyclin D1 levels were quantitated. Results showed that all these protein expression levels were changed in the vasculature and the LH to a similar degree after SAH (Supplemental Figure 4). Thus, we used LH lysates for Western blot analyses in the following studies.

PDGFR-β and IRF9 were elevated and SIRT1 was suppressed after SAH

Western blot results indicated that PDGFR-β was elevated after SAH, peaking at 12 h. Its expression level had returned to baseline levels by 72 h. IRF9 levels, hypothesized to be a downstream factor of PDGFR-β, were also elevated after SAH, similar to PDGFR-β. Interestingly, SIRT-1 was downregulated following SAH, indicating a suppressed endogenous anti-inflammatory mechanism (Figure 1). In accordance with a previous study,[14] these time course results suggest that the induction of the proinflammatory PDGFR-β signaling cascade coincides with VSMCs phenotypic transformation.

After the IRF9 and SIRT1 antibodies were verified (Supplemental Figure 7), immunofluorescence was performed to further verify that these proteins were expressed on the VSMCs. Pial arterioles with one or two smooth muscle layers were dissected and immunostained for PDGFR-β, IRF9 and SIRT1. All those proteins are co-localized with α-SMA, a VSMC marker, indicating that they are all expressed on the arteriolar VSMCs (Figure 2).

Administration of resveratrol decreased brain edema and improved neurological score 24 h after SAH

Three different dosages of the SIRT1 activator resveratrol (10, 30, 90 mg/kg) were administrated intraperitoneally (i.p.) 1 h after SAH. SAH grade, brain water content, neurological score, and beam balance were evaluated 24 h after SAH. There was no significant difference in SAH grades between vehicle (SAH + dimethyl sulfoxide, DMSO) and treatment groups (Figure 3(a)). Both medium and high doses of

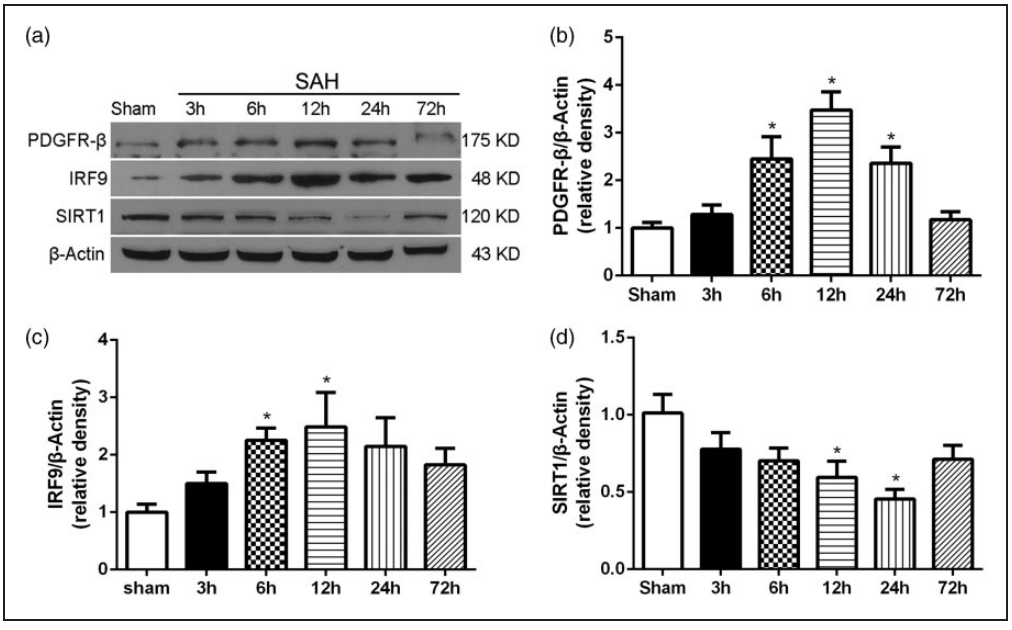

Figure 1. Platelet-derived growth factor receptor-β (PDGFR-β) and interferon regulatory factor 9 (IRF9) were upregulated, and SIRT1 is downregulated following subarachnoid hemorrhage (SAH) injury. (a) Western blot assay for the expression profiles of PDGFR-β, IRF9, SIRT1 in the whole brain of sham and SAH rats at 3, 6, 12, 24, 72 h after the operation. (b, c, d) Quantitative analysis of PDGFR-β, IRF9, SIRT1 time course after SAH. Relative densities have been normalized against the sham group. N = 6. Error bars represent mean ± SEM.* $p < 0.05$ vs. sham.

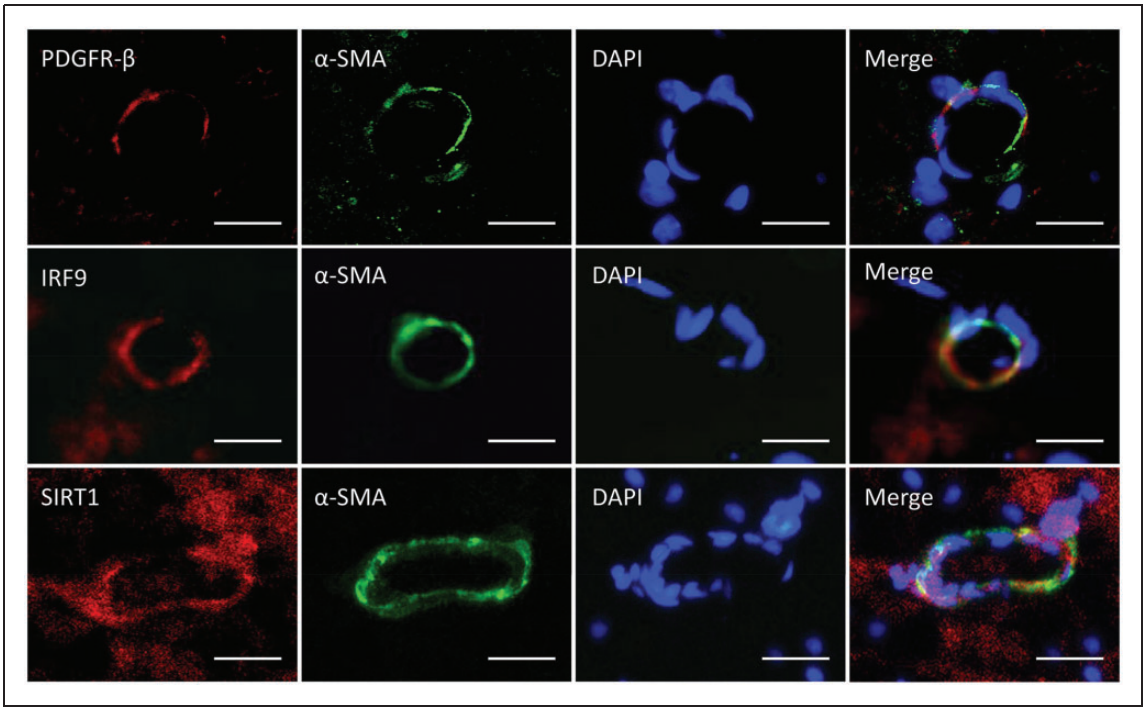

Figure 2. Immunofluorescence staining for PDGFR-β (red), IRF9 (red) and SIRT1 (red) expression on vascular smooth muscle cells (α-SMA, green) in the pial arterioles. Scale bar = 40 μm. N = 2.

resveratrol (30, 90 mg/kg) improved neurological test and beam balance scores (Figure 3(c) and (d)) 24 h after SAH. The medium dose of resveratrol (30 mg/kg) also effectively decreased brain water content (Figure 3(b)) 24 h after SAH. The results indicated that the medium and high doses of resveratrol were effective in attenuating EBI and improving neurological function after SAH. Thus, we selected the medium dosage (30 mg/kg) of resveratrol for the following studies.

PDGFR-β siRNA downregulated IRF9 expression, thus restoring SIRT1 level

PDGFR-β expression was knocked down efficiently with the i.c.v. administration of PDGFR-β siRNA compared with SAH + scrambled siRNA groups 24 h after SAH (Figure 4(b)). PDGFR-β siRNA inhibited IRF9 expression and thus restored SIRT1 expression. The administration of resveratrol had no effect on the expression levels of PDGFR-β, IRF9 and SIRT1 compared with SAH + PDGFR-β siRNA + DMSO group 24 h after SAH (Figure 4).

PDGFR-β siRNA and resveratrol conferred protective effects 24 h after SAH that were abolished by a SIRT1 inhibitor (EX527)

To further investigate the potential relationship between PDGFR-β and SIRT1, we administrated PDGFR-β siRNA or scrambled siRNA, a SIRT1 activator (resveratrol) and a SIRT1 inhibitor (EX527) in SAH rats. PDGFR-β siRNA significantly attenuated brain edema and ameliorated neurological deficits compared with the SAH + scrambled siRNA group 24 h after SAH. Similar to PDGFR-β siRNA, resveratrol also significantly attenuated brain edema and improved neurological scores. EX527 (10 mg/kg, i.p.), however, exacerbated brain edema of the LH and deteriorated neurological dysfunction compared with SAH + PDGFR-β siRNA + DMSO/ SAH + PDGFR-β siRNA + resveratrol/SAH + resveratrol (Figure 5(a) and (b)).

To verify the role of PDGFR-β in arteriolar VSMC phenotypic switching, pial arterioles with one or two smooth muscle layers were dissected and prepared for immunofluorescence. The specificity of α-SMA and Smemb antibodies was verified (Supplemental Figure 7). Staining for α-SMA (contractile phenotype marker) and Smemb (synthetic phenotype marker) was performed on sections from animals in the sham, SAH + DMSO and SAH + PDGFR-β siRNA + DMSO groups. Smemb immunoreactivity was increased in SAH animals compared to sham, and PDGFR-β siRNA effectively decreased its expression. However, α-SMA expression was suppressed after SAH and PDGFR-β siRNA restored its expression on the pial arterioles (Figure 5(c) and (d)). The immunofluorescence results indicate that VSMCs switch phenotypes after SAH, and that this process is mediated by the PDGFR-β signaling pathway.

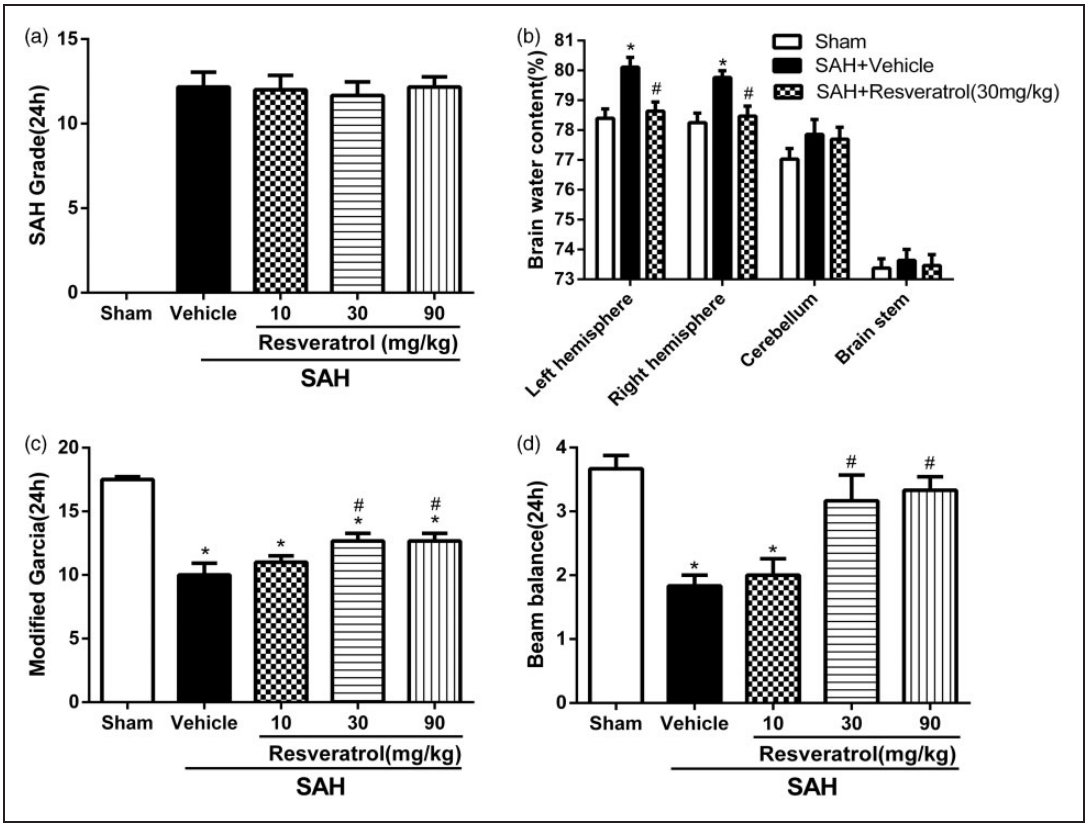

Figure 3. SIRT1 activator, resveratrol (RSV), attenuates neurological deficits and alleviates brain edema 24 h after SAH. Statistical analysis of SAH grading at 24 h after the surgery (a), brain edema (b), neurological function (c, d). N = 6. Error bars represent mean ± SEM. $^{*}p < 0.05$ vs. sham, $^{\#}p < 0.05$ vs. SAH + Vehicle.

PDGFR-β siRNA inhibited VSMC phenotypic transformation after SAH

The knockdown of PDGFR-β by siRNA remarkably downregulated the expression of the inflammatory marker NF-κB (Figure 6(b)). The proliferation marker Cyclin D1 was also decreased in a similar manner (Figure 6(d)). However, PDGFR-β siRNA upregulated the VSMC contractile phenotypic marker α-SMA significantly compared with SAH + scrambled siRNA groups 24 h after SAH (Figure 6(c)). Resveratrol did not confer further beneficial effects compared to the SAH + PDGFR-β siRNA + DMSO group. However, Ex527, a SIRT1 inhibitor, abolished the protective effects of SIRT1 compared with SAH + PDGFR-β siRNA + resveratrol groups at 24 h after SAH, indicating that SIRT1 is an essential mediator of all the beneficial effects (Figure 6).

IRF9 in vivo knockdown and SIRT1 activation preserve VSMCs contractile phenotype and suppress inflammation after SAH

To further investigate the downstream signaling cascade of PDGFR-β, IRF9 siRNA was administrated i.c.v., and the knockdown efficiency was validated by Western blot analysis. Protein expression of IRF9 significantly decreased with IRF9 siRNA administration compared with the SAH + scrambled siRNA group, whereas the level of SIRT1 remarkably increased (Supplemental Figure 5). IRF9 knockdown significantly decreased inflammation (NF-κB) and cell proliferation (Cyclin D1). The SIRT1 activator resveratrol did not provide further protective effects, whereas the SIRT1 inhibitor EX527 reversed all the beneficial effects from IRF9 knockdown. This data further indicated that SIRT1 is a downstream factor that can be inhibited by IRF9 (Supplemental Figure 6).

Discussion

SAH remains one of the most devastating hemorrhagic stroke types in the clinical setting. Vasospasm is a common complication of SAH and usually leads to delayed cerebral ischemia (DCI). In addition to vasospasm, other factors such as cortical spreading depression, microcirculatory constriction and thrombosis contribute to DCI.[8,26] Calcium channel blockers such as nimodipine and verapamil are used to reduce vasospasm and its associated ischemia in animal models and clinical management.[8,27] However, the effectiveness of

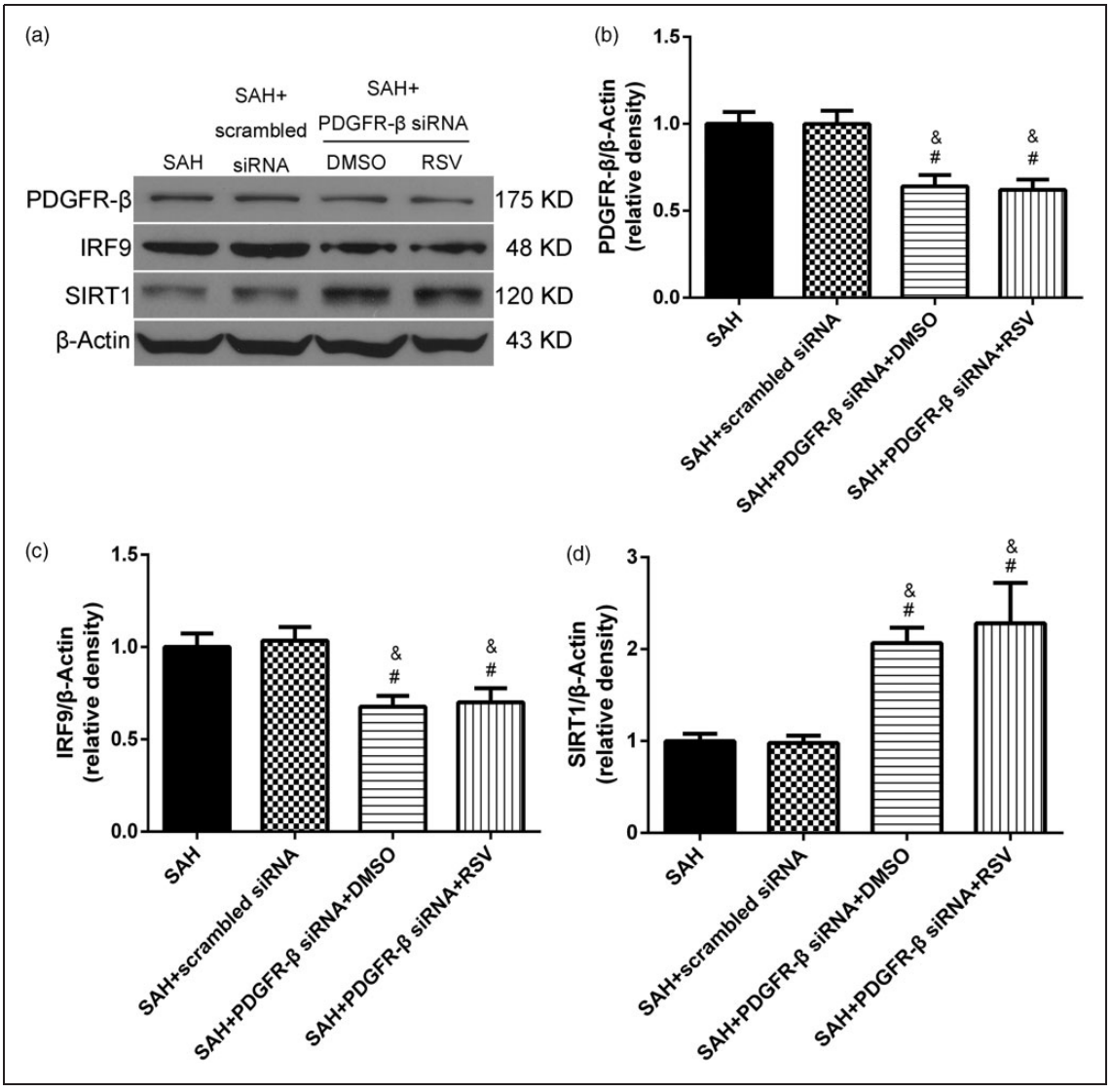

Figure 4. PDGFR-β siRNA downregulated the expression of PDGFR-β and IRF9, but upregulated the expression of SIRT1. (a) Representative blots for PDGFR-β, IRF9 and SIRT1 in indicated groups. (b, c, d) Quantitative analysis of PDGFR-β, IRF9 and SIRT1 in indicated groups. Relative densities have been normalized against the sham group. N = 6. Error bars represent mean ± SEM. $^{\#}p < 0.05$ vs. SAH + vehicle, $^{\&}p < 0.05$ vs. SAH + scrambled siRNA.

this therapeutic strategy still remains controversial.[8] Recent trends in the SAH research community suggest that efforts have shifted significantly from delayed CVS to EBI.[28] Under normal physiological conditions, VSMCs in the contractile phenotype play an essential role in regulating vascular tone. In response to injury or inflammatory stimuli, VSMCs proliferate, secrete matrix metalloproteases (MMPs), and re-synthesize ECM, all of which are the features of VSMC synthetic phenotype.[11] Thus, VSMCs may undergo phenotypic transformation from the contractile phenotype to the synthetic phenotype and lose autoregulatory capacity during the EBI phase of SAH, making vascular tone difficult to regulate with pharmacological interventions. In the long term, the vasculature (especially the microcirculation) has a thicker and stiffer vessel wall with reduced autoregulatory capacity.[10] Thus, preventing the phenotypic transformation of VSMC during EBI can be critical in alleviating DCI in SAH.

The vascular neural network highlights the role of VSMCs and presents a novel therapeutic strategy for stroke treatments.[29] A previous study from our laboratory showed that VSMCs switch from the contractile phenotype to the synthetic phenotype after SAH. It has been shown that VSMC phenotypic transformation from contractile to synthetic occurs as early as 6 h after SAH, and that preventing shift can ameliorate neurological deficits in SAH.[14] However, our previous

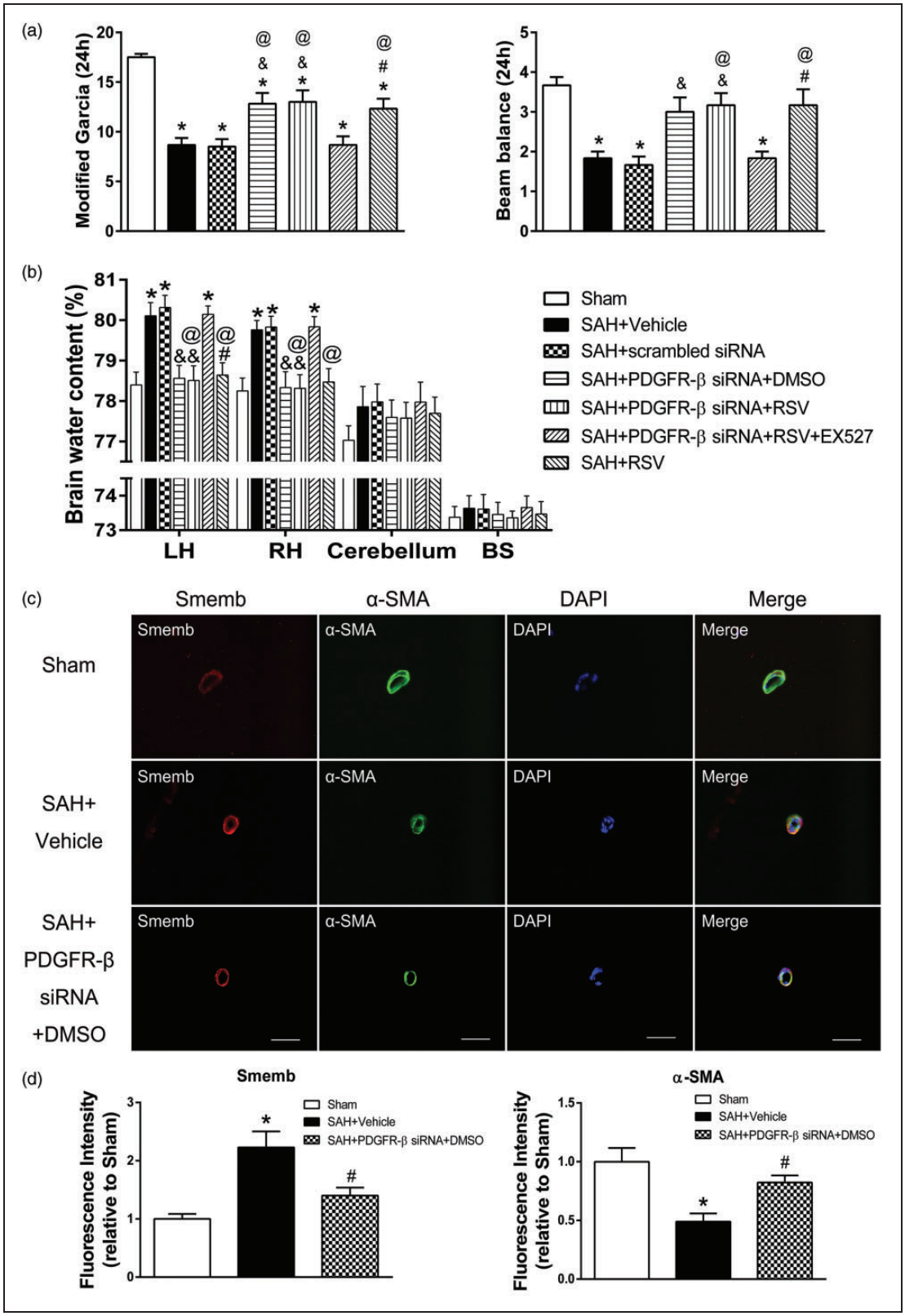

Figure 5. PDGFR-β siRNA conferred protective effects 24 h after SAH that were mediated by SIRT1. (a, b) PDGFR-β siRNA ameliorates neurological dysfunction and decreases brain edema. However, SIRT1 inhibitor EX527 abolishes those effects. (c) Representative images of immunofluorescence staining for α-SMA and Smemb in sham, SAH, SAH + PDGFR-β siRNA groups. (d) Fluorescence intensity analysis of Smemb and α-SMA in different groups. Scale bars = 50 μm. N = 6. Error bars represent mean ± SEM. *$p < 0.05$ vs. sham, $^{\#}$ $p < 0.05$ vs. SAH + vehicle. $^{\&}p < 0.05$ vs. SAH + scrambled siRNA, $^{@}p < 0.05$ vs. SAH + PDGFR-β siRNA + resveratrol + EX527.

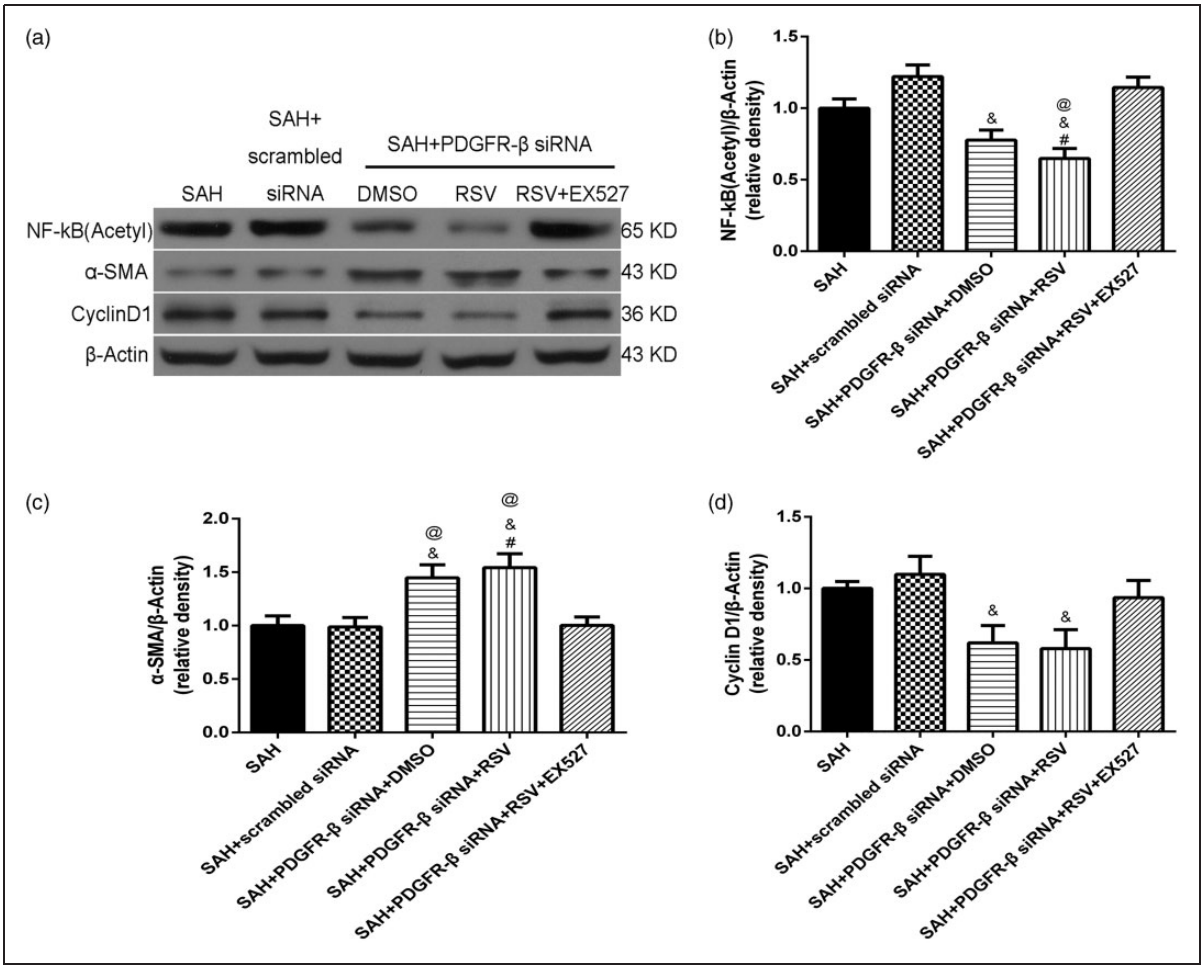

Figure 6. The beneficial effects of PDGFR-β siRNA in preserving contractile VSMCs are mediated by SIRT1. (a) Representative blots of inflammatory marker NF-κB (Acetyl), VSMC contractile marker α-SMA and proliferative marker CyclinD1. (b, c, d) Quantitative analysis of NF-κB (Acetyl), α-SMA and Cyclin D1 in SAH, SAH + scrambled siRNA, SAH + PDGFR-β siRNA + DMSO, SAH + PDGFR-β siRNA + resveratrol, SAH + PDGFR-β siRNA + resveratrol + EX527 group at 24 h following SAH. Relative densities have been normalized against the SAH group. N = 6. Error bars represent mean ± SEM. $^{\#}p < 0.05$ vs. SAH, $^{\&}p < 0.05$ vs. SAH + scrambled siRNA, $^{@}p < 0.05$ vs. SAH + PDGFR-β siRNA + resveratrol + EX527.

study focused on large cerebral arteries on the ventral surface of the brain. It remains uncertain if cerebral arterioles at a greater distance from the origin of the bleed, would exhibit a similar phenotypic transformation. In addition, very small cerebral arteries and arterioles typically have fewer layers of smooth muscle, slower blood velocity and shear stress, and greater access to metabolites and vascular growth factors released from the brain parenchyma. Recent studies have focused on the role of arterioles and microcirculation in the development of vasospasm after SAH.[23,30–32] Thus, we assessed pial arteriole VSMC phenotypic transformation in this study. In addition, another study from our laboratory characterized VSMC phenotype switching in the perihematoma area following intracerebral hemorrhage (ICH). This study showed that the PDGF-BB/PDGFR-β system contributes to VSMC phenotypic transformation via p38 mitogen-activated protein kinase (MAPK). Inhibition of PDGFR-β by Gleevec and PDGFR-β siRNA effectively preserved the VSMC contractile phenotype and alleviated neuroinflammation in the basal ganglia following ICH.[21] Another study from our laboratory shows that ICH significantly increased passive diameters of cerebral blood vessels compared to sham animals and that PDGFR-β inhibitor imatinib eliminated these differences. In addition, ICH significantly depressed incremental compliance and treatment with imatinib eliminated this effect. This study shows that PDGFR-β signaling plays a role in the cerebrovascular phenotypic transformation as demonstrated by the vascular contractility data.[33] Thus, we continue to explore the role of PDGFR-β signaling in the SAH model in the present study.

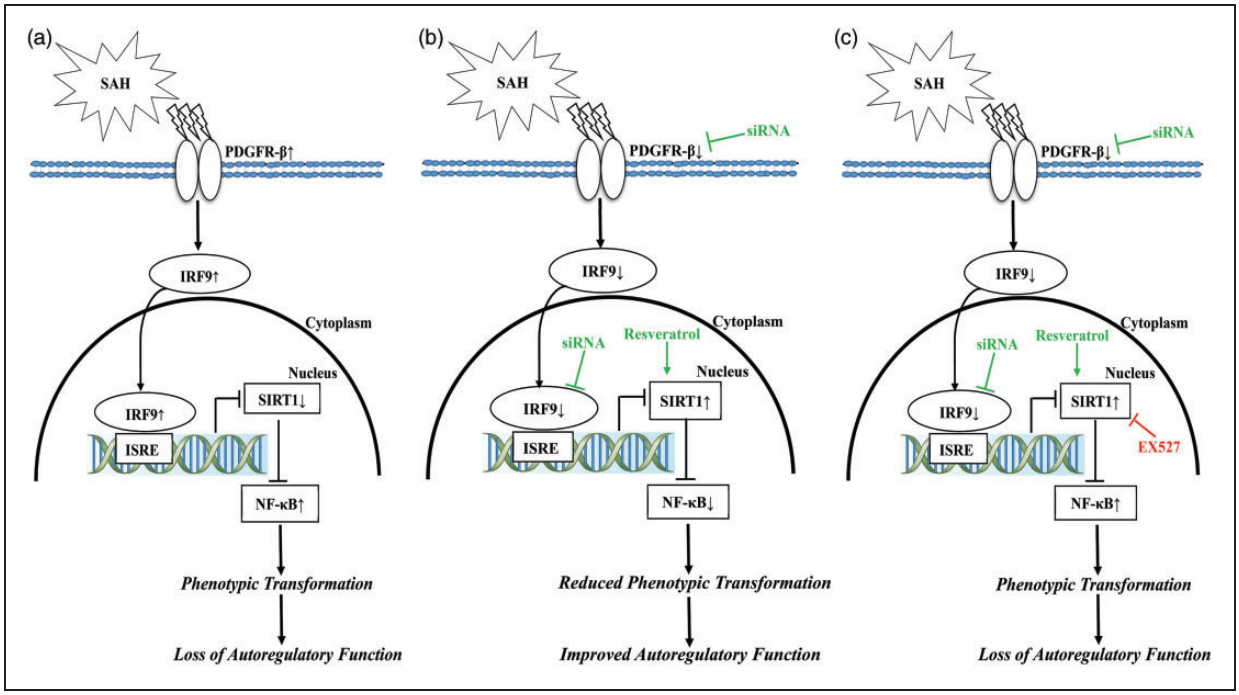

Figure 7. The schematic summary of the study. (a) SAH triggers the activation of PDGFR-β/IRF9/SIRT-1/NF-κB pathway, leading to loss of autoregulatory function of the vasculature. (b) PDGFR-β siRNA, IRF9 siRNA and resveratrol improve vascular function by promoting SIRT1. (c) SIRT1 inhibitor EX527 reverses the beneficial effects of PDGFR-β siRNA, IRF9 siRNA and resveratrol.

We hypothesized that the IRF9/SIRT1 axis is an important downstream mediator in PDGFR-β signaling. IRF9 is a transcription factor that is activated in response to proinflammatory stimuli. A previous report showed that IRF9 is upregulated in the carotid artery injury as a downstream factor of PDGF-BB signaling. Furthermore, it plays a role in the vascular injury by suppressing SIRT1 expression and activity.[18] SIRT1 is a histone deacetylase that regulates cell proliferation and suppresses inflammatory response. A previous study reported that its activator resveratrol attenuated vascular narrowing at 72 h post-SAH.[34] This same study also demonstrated that in resveratrol-treated rats, both brain and serum endothelin-1 levels were decreased compared to the non-treated group. Interestingly, another study showed that PDGFR-β mediated VSMC proliferation as a downstream factor of endothelin-1 in pulmonary vascular remodeling.[35] If this also holds true in the cerebral vasculature, it is deducible that the decrease in endogenous SIRT1 level can result in further increase of endothelin-1 and further activation of PDGFR-β, forming a positive feedback loop. Thus, exogenous resveratrol can be potentially important in preventing the formation of this loop. The "IRF9-SIRT1 axis" has been shown to play an essential role in neointima formation upon carotid vascular injury and may be a potential novel therapeutic target. Thus, we examined whether this axis also plays a role in the vascular injury SAH, connecting PDGFR-β and SIRT1. Our data showed that resveratrol conferred beneficial effects, as demonstrated by improved neurological test and beam balance scores. Resveratrol also attenuated brain edema 24 h after SAH. Our time course results indicated that IRF9 expression is upregulated after SAH, following the increasing trend of PDGFR-β. Interestingly, SIRT1 expression is downregulated, showing a negative temporal correlation with both PDGFR-β and IRF9. In addition, the synthetic VSMC marker Smemb was induced as early as 6 h after SAH and continued to increase at 72 h.[14] To further validate this signaling pathway, we employed both PDGFR-β siRNA and IRF9 siRNA to examine the expression of downstream signaling mediators and outcomes. Our results show that knockdown of both proteins restored expression of SIRT1 and significantly reduced the inflammatory marker NF-κB and proliferation marker Cyclin D1, all of which indicated the protective effects of silencing PDGFR-β and IRF9. These results suggest that PDGFR-β/IRF9 activation inhibits SIRT1, an endogenous anti-inflammatory factor, and that the silencing of upstream factors restored this protective mechanism. However, all of these beneficial effects were abolished by the SIRT1 inhibitor EX527, thus validating that SIRT1 is the key mediator in maintaining VSMCs contractile phenotype (Figure 7).

One of the limitations of this study is that we only investigated males in this study. Since females,

especially postmenopausal females, are at higher risk for SAH and have larger lesions after SAH in EBI.[36–38] It would be important and intriguing to validate this pathway in females.

This study demonstrated that the PDGFR-β/IRF9/SIRT1 signaling pathway mediates VSMC phenotypic transformation during EBI after SAH. The inhibition of PDGFR-β and IRF9 or the activation of SIRT1 preserved contractile VSMCs, attenuated brain edema, and improved neurological function after SAH. Our study is also the first to demonstrate phenotypic transformation of VSMC in the arterioles, providing a novel therapeutic strategy for SAH.

Funding

The author(s) disclosed receipt of the following financial support for the research, authorship, and/or publication of this article: This research was supported by the National Institute of Health grant P01NS082184 to Dr. Zhang and the grant from National Natural Science Foundation of China (81371319).

Declaration of conflicting interests

The author(s) declared no potential conflicts of interest with respect to the research, authorship, and/or publication of this article.

Authors' contributions

Weifeng Wan brought up the concept, performed the experiments and drafted the manuscript. Yan Ding did experimental design and manuscript preparation. Zongyi Xie and Feng Yan performed neurobehavioral studies. Qian Li assisted experiments. Enkhjargal Budbazar participated in the experimental design. William. Pearce, Richard Hartman and Andre Obenaus revised the manuscript. Weifeng Wan and Yan Ding worked on the manuscript revision. John H. Zhang, Yong Jiang and Jiping Tang conceived, designed and coordinated the study.

Supplementary material

Supplementary material for this paper can be found at the journal website: http://journals.sagepub.com/home/jcb

ORCID iD

John H Zhang http://orcid.org/0000-0002-4319-4285

References

1. Friedrich B, Muller F, Feiler S, et al. Experimental subarachnoid hemorrhage causes early and long-lasting microarterial constriction and microthrombosis: an in-vivo microscopy study. *J Cereb Blood Flow Metab* 2012; 32: 447–455.
2. Hasan D, Vermeulen M, Wijdicks EF, et al. Management problems in acute hydrocephalus after subarachnoid hemorrhage. *Stroke* 1989; 20: 747–753.
3. Busch E, Beaulieu C, de Crespigny A, et al. Diffusion MR imaging during acute subarachnoid hemorrhage in rats. *Stroke* 1998; 29: 2155–2161.
4. Liu Y, Soppi V, Mustonen T, et al. Subarachnoid hemorrhage in the subacute stage: elevated apparent diffusion coefficient in normal-appearing brain tissue after treatment. *Radiology* 2007; 242: 518–525.
5. Cahill J, Calvert JW and Zhang JH. Mechanisms of early brain injury after subarachnoid hemorrhage. *J Cereb Blood Flow Metab* 2006; 26: 1341–1353.
6. Claassen J, Carhuapoma JR, Kreiter KT, et al. Global cerebral edema after subarachnoid hemorrhage: frequency, predictors, and impact on outcome. *Stroke* 2002; 33: 1225–1232.
7. Munakata A, Naraoka M, Katagai T, et al. Role of cyclooxygenase-2 in relation to nitric oxide and endothelin-1 on pathogenesis of cerebral vasospasm after subarachnoid hemorrhage in rabbit. *Transl Stroke Res* 2016; 7: 220–227.
8. Macdonald RL. Delayed neurological deterioration after subarachnoid haemorrhage. *Nat Rev Neurol* 2014; 10: 44–58.
9. Alexander MR and Owens GK. Epigenetic control of smooth muscle cell differentiation and phenotypic switching in vascular development and disease. *Annu Rev Physiol* 2012; 74: 13–40.
10. Shimamura N and Ohkuma H. Phenotypic transformation of smooth muscle in vasospasm after aneurysmal subarachnoid hemorrhage. *Transl Stroke Res* 2014; 5: 357–364.
11. Hao H, Gabbiani G and Bochaton-Piallat ML. Arterial smooth muscle cell heterogeneity: implications for atherosclerosis and restenosis development. *Arterioscler Thromb Vasc Biol* 2003; 23: 1510–1520.
12. Campbell GR and Campbell JH. The phenotypes of smooth muscle expressed in human atheroma. *Ann N Y Acad Sci* 1990; 598: 143–158.
13. Thyberg J, Blomgren K, Hedin U, et al. Phenotypic modulation of smooth muscle cells during the formation of neointimal thickenings in the rat carotid artery after balloon injury: an electron-microscopic and stereological study. *Cell Tissue Res* 1995; 281: 421–433.
14. Wu J, Zhang Y, Yang P, et al. Recombinant osteopontin stabilizes smooth muscle cell phenotype via integrin receptor/integrin-linked kinase/rac-1 pathway after subarachnoid hemorrhage in rats. *Stroke* 2016; 47: 1319–1327.
15. Shiba M, Suzuki H, Fujimoto M, et al. Imatinib mesylate prevents cerebral vasospasm after subarachnoid hemorrhage via inhibiting tenascin-C expression in rats. *Neurobiol Dis* 2012; 46: 172–179.
16. Shiba M, Suzuki H, Fujimoto M, et al. Role of platelet-derived growth factor in cerebral vasospasm after subarachnoid hemorrhage in rats. *Acta Neurochir Suppl* 2013; 115: 219–223.
17. Zhang XJ, Zhang P and Li H. Interferon regulatory factor signalings in cardiometabolic diseases. *Hypertension* 2015; 66: 222–247.
18. Zhang SM, Zhu LH, Chen HZ, et al. Interferon regulatory factor 9 is critical for neointima formation following vascular injury. *Nat Commun* 2014; 5: 5160.

19. Shah SA, Khan M, Jo MH, et al. Melatonin stimulates the SIRT1/Nrf2 signaling pathway counteracting lipopolysaccharide (LPS)-induced oxidative stress to rescue postnatal rat brain. *CNS Neurosci Ther* 2017; 23: 33–44.
20. Guo Z, Hu Q, Xu L, et al. Lipoxin A4 reduces inflammation through formyl peptide receptor 2/p38 MAPK signaling pathway in subarachnoid hemorrhage rats. *Stroke* 2016; 47: 490–497.
21. Yang P, Wu J, Miao L, et al. Platelet-derived growth factor receptor-beta regulates vascular smooth muscle cell phenotypic transformation and neuroinflammation after intracerebral hemorrhage in mice. *Crit Care Med* 2016; 44: e390–e402.
22. Sugawara T, Ayer R, Jadhav V, et al. A new grading system evaluating bleeding scale in filament perforation subarachnoid hemorrhage rat model. *J Neurosci Meth* 2008; 167: 327–334.
23. Tso MK and Macdonald RL. Subarachnoid hemorrhage: a review of experimental studies on the microcirculation and the neurovascular unit. *Transl Stroke Res* 2014; 5: 174–189.
24. Lee MH, Kwon BJ, Seo HJ, et al. Resveratrol inhibits phenotype modulation by platelet derived growth factor-bb in rat aortic smooth muscle cells. *Oxidative Med Cell Longev* 2014; 2014: 572430.
25. Zhang Y, Chen Y, Wu J, et al. Activation of dopamine D2 receptor suppresses neuroinflammation through alphaB-crystalline by inhibition of NF-kappaB nuclear translocation in experimental ICH mice model. *Stroke* 2015; 46: 2637–2646.
26. Vergouwen MD, Ilodigwe D and Macdonald RL. Cerebral infarction after subarachnoid hemorrhage contributes to poor outcome by vasospasm-dependent and -independent effects. *Stroke* 2011; 42: 924–929.
27. Marbacher S, Neuschmelting V, Graupner T, et al. Prevention of delayed cerebral vasospasm by continuous intrathecal infusion of glyceroltrinitrate and nimodipine in the rabbit model in vivo. *Intens Care Med* 2008; 34: 932–938.
28. Marbacher S. Animal models for the study of subarachnoid hemorrhage: are we moving towards increased standardization? *Transl Stroke Res* 2016; 7: 1–2.
29. Zhang JH, Badaut J, Tang J, et al. The vascular neural network – a new paradigm in stroke pathophysiology. *Nat Rev Neurol* 2012; 8: 711–716.
30. Naraoka M, Matsuda N, Shimamura N, et al. The role of arterioles and the microcirculation in the development of vasospasm after aneurysmal SAH. *Biomed Res Int* 2014; 2014: 253746.
31. Atangana E, Schneider UC, Blecharz K, et al. Intravascular inflammation triggers intracerebral activated microglia and contributes to secondary brain injury after experimental subarachnoid hemorrhage (eSAH). *Transl Stroke Res* 2017; 8: 144–156.
32. Terpolilli NA, Feiler S, Dienel A, et al. Nitric oxide inhalation reduces brain damage, prevents mortality, and improves neurological outcome after subarachnoid hemorrhage by resolving early pial microvasospasms. *J Cereb Blood Flow Metab* 2016; 36: 2096–2107.
33. Pearce WJ, Doan C, Carreon D, et al. Imatinib attenuates cerebrovascular injury and phenotypic transformation after intracerebral hemorrhage in rats. *Am J Physiol Regul Integr Comp Physiol* 2016; 311: R1093–R1104.
34. Karaoglan A, Akdemir O, Barut S, et al. The effects of resveratrol on vasospasm after experimental subarachnoidal hemorrhage in rats. *Surg Neurol* 2008; 70: 337–343.
35. Jankov RP, Kantores C, Belcastro R, et al. A role for platelet-derived growth factor beta-receptor in a newborn rat model of endothelin-mediated pulmonary vascular remodeling. *Am J Physiol Lung Cell Mol Physiol* 2005; 288: L1162–L1170.
36. Guo D, Wilkinson DA, Thompson BG, et al. MRI characterization in the acute phase of experimental subarachnoid hemorrhage. *Transl Stroke Res* 2017; 81: 234–243.
37. Turan N, Heider RA, Zaharieva D, et al. Sex differences in the formation of intracranial aneurysms and incidence and outcome of subarachnoid hemorrhage: review of experimental and human studies. *Transl Stroke Res* 2016; 7: 12–19.
38. Ahnstedt H, McCullough LD and Cipolla MJ. The importance of considering sex differences in translational stroke research. *Transl Stroke Res* 2016; 7: 261–273.